CHEMBIOCHEM

DOI: 10.1002/cbic.200900621

Crystal Structure of the Human Monoacylglycerol Lipase, a Key Actor in Endocannabinoid Signaling

Geoffray Labar,[a] Cédric Bauvois,[b] Franck Borel,[c] Jean-Luc Ferrer,[c] Johan Wouters,[d] and Didier M. Lambert*[a]

This article is dedicated to the memory of Dr. Lilian Jacquamet, from the research group in Grenoble, who unexpectedly passed away during the course of this work.

2-Arachidonoylglycerol plays a major role in endocannabinoid signaling, and is tightly regulated by the monoacylglycerol lipase (MAGL). Here we report the crystal structure of human MAGL. The protein crystallizes as a dimer, and despite structural homologies to haloperoxidases and esterases, it distinguishes itself by a wide and hydrophobic access to the catalytic site. An apolar helix covering the active site also gives structural insight into the amphitropic character of MAGL, and likely explains how MAGL interacts with membranes to recruit its substrate. Docking of 2-arachidonoylglycerol highlights a hydrophobic and a hydrophilic cavity that accommodate the lipid into the catalytic site. Moreover, we identified Cys201 as the crucial residue in MAGL inhibition by *N*-arachidonylmaleimide, a sulfhydryl-reactive compound. Beside the advance in the knowledge of endocannabinoids degradation routes, the structure of MAGL paves the way for future medicinal chemistry works aimed at the design of new drugs exploiting 2-arachidonoylglycerol transmission.

Introduction

Fatty acids are essential to life. Their contributions range from providing energy stores and precursors of cell membrane constituents to binding to nuclear receptors in order to modulate gene transcription. In addition, several lipids, termed endocannabinoids, were identified in the nineties as new molecular messengers. These bind to and activate the CB_1 and CB_2 cannabinoid receptors,[1,2] the molecular targets for the main *Cannabis sativa* L. psychoactive compound, Δ^9-THC. Along with anandamide,[3] 2-arachidonoylglycerol (2-AG)[4,5] mediates retrograde signaling[6] and plays a major role in the endocannabinoid system.

Beside the regulation of anandamide tone by the fatty acid amide hydrolase (FAAH), regulation of 2-AG degradation pathways also constitutes a major challenge for both understanding the endocannabinoid system and for therapeutic purposes.[7–9] 2-AG acts as a retrograde messenger to modulate synaptic transmission, and different pieces of evidence point towards 2-AG as the putative "true" endogenous ligand of cannabinoid receptors.[10] First of all, it is the most abundant endocannabinoid in the brain,[11] and second, unlike anandamide, it acts as a full agonist at both CB_1 and CB_2 cannabinoid receptors. 2-AG elicits a wide range of beneficial properties, among which analgesic, anti-inflammatory,[12,13] immunomodulating,[14,15] neuroprotective[16] and hypotensive effects,[17] as well as the ability to inhibit the growth of prostate and breast cancer cells.[18,19]

2-AG transmission is tightly regulated by MAGL,[20–22] an ubiquitous 33 kDa enzyme, now considered a promising target for the development of antiinflammatory and analgesic compounds.[13,23] Indeed, despite the fact that in vitro, different enzymes are able to hydrolyse 2-AG, recent evidence suggests that MAGL is the major enzyme responsible for the regulation of 2-AG levels. First, RNA silencing of MAGL in HeLa cells yields an increase in 2-AG levels in HeLa cells.[24] Second, despite the identification of two additional 2-AG hydrolases (ABHD6 and ABHD12), activity-based proteome profiling allowed assignment of 85% of the total 2-AG hydrolysis in the brain to MAGL.[22] And last, in vivo administration of JZL184, the first selective MAGL inhibitor, produces a fourfold increase in 2-AG levels, without affecting other monoacylglycerols and *N*-acylethanolamines.[13] Interestingly, JZ184, as well as OMDM169, another selective MAGL inhibitor, has displayed analgesic properties in two different models of pain in mice.[13,23]

[a] *G. Labar, Prof. D. M. Lambert*
Unité de Chimie Pharmaceutique et de Radiopharmacie (CMFA)
Louvain Drug Research Institute
Université catholique de Louvain, Faculté de Médecine
Avenue E. Mounier 73.40, 1200 Brussels (Belgium)
Fax: (+33) 3227647363
E-mail: didier.lambert@uclouvain.be

[b] *Dr. C. Bauvois*
Institut de Recherches Microbiologiques Jean-Marie Wiame (IRMW)
Avenue E. Gryson 1, 1070 Brussels (Belgium)

[c] *Dr. F. Borel, Dr. J.-L. Ferrer*
Laboratoire de Cristallographie et Cristallogenèse des Protéines
Institut de Biologie Structurale J.-P. Ebel
UMR5075 CEA-CNRS-Université J. Fourier
38027 Grenoble Cedex 1 (France)

[d] *Prof. J. Wouters*
Laboratoire de Chimie biologique structurale (CBS)
Facultés universitaires Notre-Dame de la Paix (FUNDP), Faculté des Sciences
Rue de Bruxelles 61, 5000 Namur (Belgium)

Supporting information for this article is available on the WWW under http://dx.doi.org/10.1002/cbic.200900621.

These data highlight the physiological relevance of MAGL in the regulation of 2-AG signaling. However, apart from JZL184, which was recently developed, therapeutic exploitation and fundamental knowledge of MAGL still suffer from the paucity of the inhibitors available. These lack either potency or selectivity towards FAAH or other carboxylesterases. In this context, the knowledge of MAGL tridimensional structure would constitute a precious tool to help the design of such compounds.

Here, we report the tridimensional structure of human MAGL and present the key structural features that enable the enzyme to accomplish its biological functions. Beside the in-depth knowledge of the major pathway that governs 2-AG hydrolysis, it should constitute a step forward in the race to design new pharmacological and therapeutic agents on a rational basis.

Results and Discussion

Overall fold

The structure of human MAGL was solved at 2.2 Å resolution by X-ray diffraction. The protein crystallized in I222 space group, with two molecules per asymmetric unit (Figure 1). The two monomers are in contact by a surface of 884 Å^2; this represents about 7% of the total surface of a monomer. Consistently, MAGL was found as a dimer in a mass spectrometry experiment and no peak corresponding to the monomeric protein was found after gel filtration chromatography. Moreover, both catalytic site entries face the same direction and are thus properly oriented to interact with the membrane in order to recruit the substrates, similar to what was reported following elucidation of the FAAH structure, the main enzyme responsible for anandamide catabolism.[25] Taken together, these data strongly suggest that MAGL is organized as a biological dimer.

According to secondary structure prediction,[20] MAGL architecture presents the hallmark of the α/β hydrolases superfamily. The central β-sheet, constituted of seven parallel and one antiparallel strands, is surrounded by six α helices (Figure 1). A cap domain, which varies much more among the members of this superfamily, covers the structurally conserved β-sheet and the active site. Buried below the cap is the catalytic triad, closely superimposed on that of other hydrolases and haloperoxidases, and made up of residues Ser122, Asp239 and His269. The tridimensional structure thus provides the first direct evidence of the identity of this catalytic triad, previously reported based on mutagenesis studies.[20] The Ser122 is located in the GXSXG consensus sequence, between helix α3 and strand β5, in the so-called "nucleophilic elbow" sharp turn found within this superfamily. The oxyanion hole is constituted by backbone NH from Ala51 and Met123 and stabilizes the tetrahedral anionic intermediate during hydrolysis (Figures 1 and 4).

The chloroperoxidase from *Streptomyces lividans*[26] had been previously used as a template structure to construct a homology model of MAGL.[27,28] Nevertheless, careful inspection of this protein folding, as well as that of other structural homologues (i.e., haloperoxidases,[26] esterases,[29,30] the hypothetical protein PA2218 from *Pseudomonas Aeruginosa*, gastric lipase,[31] etc.) reveals that although their central core and catalytic triad superpose very well with that of MAGL, all these structures differ much more if the cap domain (that is, from residue 151 to 225 in MAGL) and substrate binding site are considered. This is explained by the poor sequence homology between MAGL and its closest homologues, which is almost inexistent within the cap domain and reaches only 20% at best for the whole sequence. In esterases and haloperoxidases cited above, this cap consists of four α helices organized to form two superimposed V-shaped structures (Figure 2). In MAGL however, this region varies substantially. While in the upper part, the first α helix (α4) has moved ~15 Å outwards compared to chloroperoxidases,

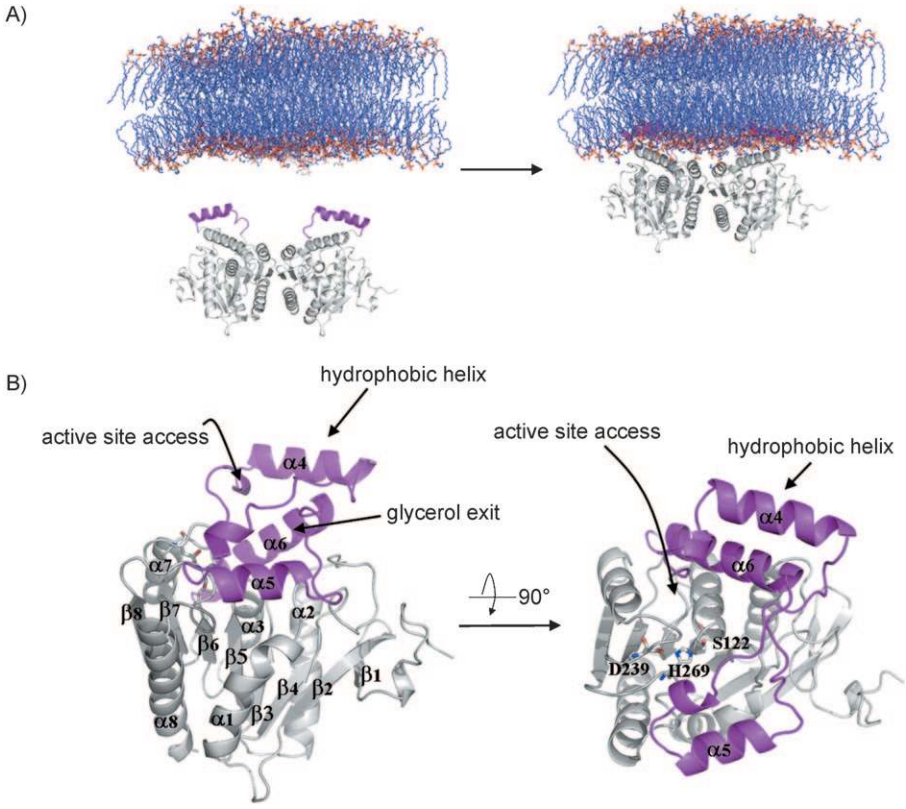

Figure 1. Overall structure of hMAGL. A) MAGL asymmetric unit. α4 helix is colored magenta. Membrane representation is a palmitoyloleoylphosphatidylethanolamine bilayer minimized using molecular dynamics simulation.[47] B) Left: Side view of a MAGL monomer, with catalytic triad represented as sticks, and cap domain colored magenta. Right: Top view (90° rotation) of the same MAGL subunit.

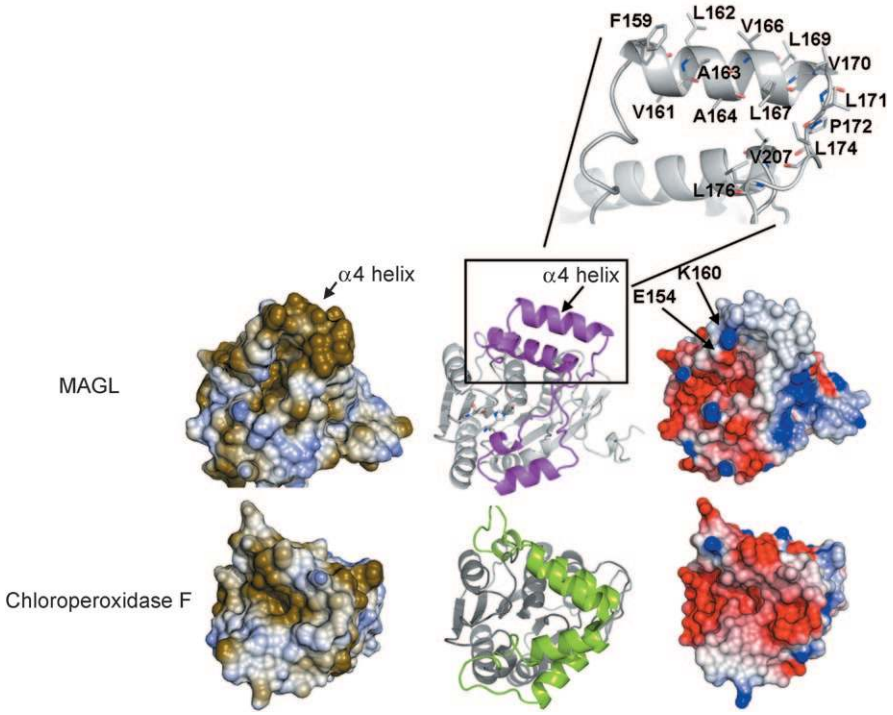

Figure 2. Comparison of the variable cap domain and active site entry of MAGL and chloroperoxidase F from *Pseudomonas fluorescens*. Middle: V-shaped organization of the chloroperoxidase cap (colored green) is clearly apparent. MAGL cap architecture (colored magenta) varies substantially. This allows MAGL cap to tend towards a more U-shaped architecture, and a wider active site access, as seen in the surface representations. Left: Surface representation, colored following lipophilic potential (VASCo software; brown: lipophilic; blue: hydrophilic; white: in between). In MAGL, the α4 helix has a marked hydrophobic character. Right: Surface representation, coloured following electrostatic potential (Delphi software; red: negative; blue: positive; white: neutral). In MAGL, the α4 helix is much more neutral than the corresponding helix in chloroperoxidase F. Top right: Magnification of this helix and its neighbourhood, with hydrophobic residues highlighted.

the second helix is absent and replaced by a long loop connecting α4 to α5 (Figure 2 and Figure S3 in the Supporting Information). Similarly, in the lower part of this cap, a longer loop (ten residues, ranging from 197 to 206, compared to three in chloroperoxidases) connects α5 to α6 helices. Through these modifications, the V-shaped organization of the four α helices of esterases and haloperoxidases is replaced by a wider U-shaped structure, and this allows MAGL to offer substrates broader access to the active site compared to related proteins. It is noteworthy that the architecture of this cap is structurally closest to that of the "hypothetical protein PA2218" from *Pseudomonas aeruginosa*, a protein of unknown function (Figure S3).

Substrate recruitment

Electrostatic and lipophilic potential surfaces highlight another major structural feature of MAGL (Figure 2). Inside the cap domain, and lining the active site access, the α4 helix is neutral and very lipophilic. Therefore, this helix defines a zone of marked hydrophobicity at the surface of MAGL. Moreover, together with residues Leu174 and Leu176, this zone lines the main part of the rim constituting the entry to the active site. In the closely related arylesterase and chloroperoxidase, the corresponding helix is charged and more hydrophilic, and therefore the surface exposed to the solvent is in accordance with the less lipophilic nature as well as the expected cytosolic localisation of their substrates (small esters and organic acids, respectively) compared to 2-AG.

It is useful here to mention that since its discovery, MAGL was sometimes considered a cytosolic enzyme and sometimes a membrane-associated one. Expression in cos-7 cells, for example, results in hydrolase activity that can be found both in the cytosol and in the membrane fraction of the cells.[21] Similarly, by using the activity-based proteome profiling technology, Cravatt's team found MAGL both in soluble and membrane mouse brain proteomes.[22] Apolar and lipophilic residues in the α4 helix neither point towards the active site nor towards the active site access, but rather towards the outside of the protein; this suggests that MAGL is present in the cell as an amphitropic enzyme and that this hydrophobic helix allows the soluble protein either to get in close contact with or to anchor in the membrane in order to reach its lipophilic substrates (Figures 1 and 2). Following this, the organization of the cap, together with the hydrophobic rim, would constitute an optimal entry for the hydrophobic and voluminous substrate 2-AG. Moreover, similarly to what was reported following elucidation of FAAH structure, three more hydrophilic residues span one of the sides of the rim that gives access to the active site. Indeed, Asn152, Glu154 and Lys160 side chains could putatively provide MAGL the means to interact through ion–dipole and dipole–dipole interactions with the polar 2-AG glycerol moiety before it plunges into the active site pocket (Figure 2). Alternatively, Lys160 might interact with negatively charged membrane phospholipids. Therefore, taken together, these particularities likely render MAGL able to recruit lipid substrates from their membrane environment and lead them to the active site to stop their action. It is also possible for a post-translational event (i.e., glycosylation, phosphorylation) to be involved in this translocation between the membrane and the cytosolic compartment. Indeed, rat and mouse brain MAGL were reported to migrate as two bands in gel electrophoresis.[21,32] Further studies are needed to clarify this.

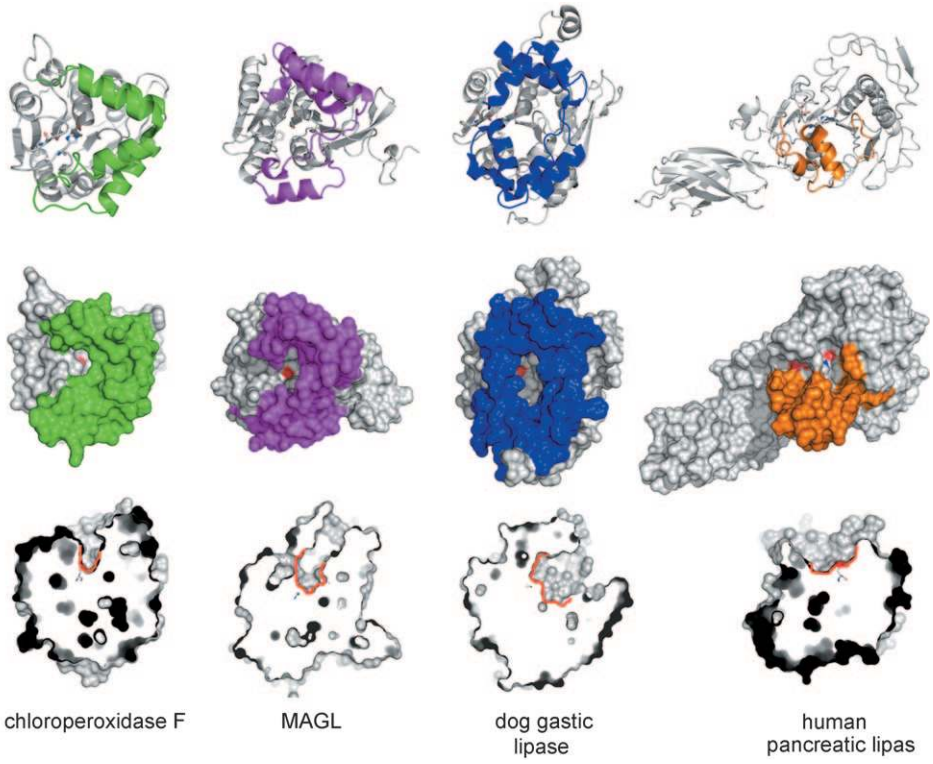

Figure 3. Through their cap organization, four α/β hydrolases have evolved to display different substrate specificities. From top to bottom: ribbon representation, surface representation (with the variable cap domain colored and nucleophilic serine in red), and transverse section highlighting the near environment of the nucleophilic serine (lined in red). From left to right: chloroperoxidase F, human MAGL, dog gastric and human pancreatic lipases. Access to the active site and to the nucleophilic serine is wider as we move from chloroperoxidase F (which acts on small organic acids) to dog gastric and human pancreatic lipases (which acts on triglycerides). In MAGL, compared to the latter two, a more restricted space near the nucleophilic serine explains its inability to hydrolyze di- and triglycerides.

Biological function of the cap

Interestingly, a comparison between MAGL and two triglyceride lipases, dog gastric and human pancreatic lipases, the structures of which have been elucidated, reveals drastic differences that are essential to explain their distinct biological functions (Figure 3).

Open forms of gastric and pancreatic lipases reveal how these proteins, while structurally distant from each other, have evolved to adopt a wider, less restricted space in the near environment of the nucleophilic serine. This likely explains their substrate specificity, and more particularly their ability to hydrolyse more voluminous substrates—that is, di- and triglycerides—compared to MAGL, which was reported to be inactive on such compounds. Considering this point, MAGL seems to be at the frontier between haloperoxidases, which act on small organic acids, and di- or tri-glyceride lipases (Figure 3).

Beside this, in these lipases, the cap domain has evolved to serve as a lid; this allows the enzymes to unveil their otherwise unreachable hydrophobic active sites if the proteins come into contact with lipid droplets. This process has been termed interfacial activation,[33] and thereby allows the enzyme to exist in two main conformational states, a closed and an open form. Along this line, it would not be surprising if this first structure of MAGL did not constitute the unique biologically relevant conformation adopted by the enzyme.

The elucidation of open structures of other lipases classically required the use of an amphiphile, an inhibitor or a lipid.[31,34,35] However, human pancreatic lipase-related protein 2 (HPLRP2) has been reported to crystallize in its open conformation without the need of a detergent or inhibitor.[36] Based on the fact that an inhibitor (E600, diethyl *p*-nitrophenyl phosphate) freely reaches the HPLRP2 active site in a detergent-free solution and on the lack of interfacial activation, the authors suggested the elegant hypothesis that the enzyme naturally adopts this conformation in solution, and related this to the HPLRP2 preference for substrates present in solution as monomers or forming small micellar aggregates.

The MAGL structure reported herein represents an "open" form, that is, a conformation that allows access to the active site. On the one hand, detergents are not required for crystallization or to allow inhibitors to access the active site. Beside this, no interfacial activation has been described for MAGL, neither is there any evidence that alternative biological conformations do exist. Taken together, this tends to support the idea that MAGL is naturally open in solution. On the other hand however, we can not totally rule out the possibility that the conformation observed here could have been facilitated or stabilized by the crystal packing or by a detergent used during the purification step—despite the fact that it is not visible in the electron density. The α4 helix in the B monomer is poorly defined; thus, this also suggests a certain flexibility.

This question is of crucial importance, and it is likely that the elucidation of other crystal forms and/or crystallization conditions will be of great value for providing insight into MAGL cap biological function and to gain information about this hypothetic conformational change that could occur in the cap if the enzyme reaches its site of action or during the substrate recognition process.

With the idea of exploring the possible existence of another lid conformation, and most importantly for drug design purposes, we tried to obtain the structure of enzyme–inhibitor complexes. However, crystal soaking was unsuccessful, as no electron density corresponding to the compound could be

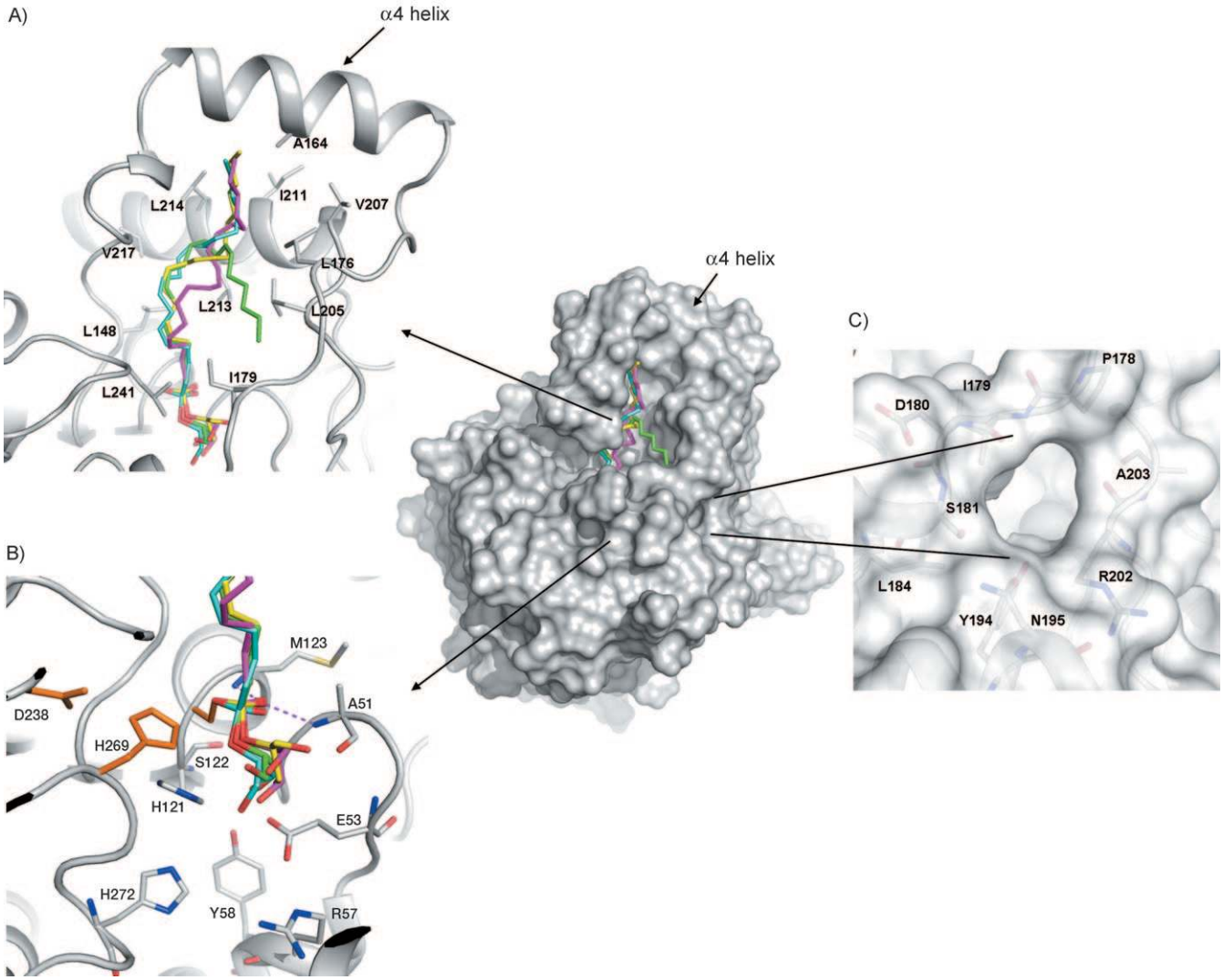

Figure 4. Docking of 2-AG in the active site of MAGL. The natural substrate is bound in the tetrahedral intermediate state to Ser122. The four first conformations found by using Gold software are represented using different colours. A) Acyl-binding and B) alcohol-binding sites are highlighted, as well as C) the glycerol exit channel. Side chains of residues interacting with the 2-AG acyl moiety or lining the hydrophilic cavity are represented as sticks. The interactions in the oxyanion hole are represented with dashed lines. The α4 helix is also indicated by arrows.

detected in the electron density map. Labelling the protein with LY2183240 or MAFP during the purification process, as well as cocrystallization experiments, also failed to produce crystals. The reasons for this are unclear. In the crystal soaking experiment, this might reflect an inaccessibility of the active site due to crystal packing. However, as our attempts to crystallize the enzyme previously bound to the inhibitors also failed, this could precisely constitute an argument towards the idea of a conformational change. Supporting this latter hypothesis is the fact that the hydrophobic α4 helix is involved in crystal packing. Therefore, if such a conformational change, even subtle, occurs following the binding of an inhibitor, it is likely that this event would be enough to prevent the crystal growth.

Binding of the natural substrate

Elucidation of the MAGL structure provides the first structural basis for rational drug design. To illustrate this and to highlight some key structural features of the active site, 2-AG has been docked in MAGL, simulating the tetrahedral intermediate state covalently bound to Ser122 Oγ (Figure 4). This reveals a cavity able to accommodate the long and flexible lipid chain of the substrates. This cavity becomes wider as one moves away from the catalytic triad environment, deeply buried in the protein, to the surface of the protein. Several hydrophobic residues cover the channel leading from the surface to the nucleophilic serine. Indeed, Leu148, Ala164, Leu176, Ile179, Leu205, Val207, Ile211, Leu213, Leu214, VaL217 and Leu241 side chains are properly located to interact with the arachidonoyl moiety of 2-AG, and mediate the MAGL substrate specificity for lipid substrates.

The near environment of the catalytic triad presents a more hydrophilic character than the channel pointing towards the enzyme surface. Besides the backbone NH from Met123 and Ala51, which form the "oxyanion hole," the Tyr58 hydroxyl group, the NH from the His121 and His272 side chains, the guanidinium from Arg57, the carboxylate from Glu53, and the backbone carbonyl from Ala51 delimit a polar cavity that accommodates the polar glycerol head group of 2-AG. A glycerol molecule found in this alcohol-binding pocket is in support of the proposed binding mode of 2-AG. A positive electron density feature was apparent in the vicinity of the oxyanion hole at the end of the structure-refinement process. This was located at the entry of this polar cavity and precisely at the same place as the glycerol moiety in 2-AG docking results. A glycerol molecule, used as a cryoprotectant after the purification procedure, was found to fit nicely in this region of high positive electron density, and therefore gives us an insight into substrate–enzyme interactions in the alcohol-binding cleft (Figure 5). The glycerol alcohol moieties are in interaction with the Ala51 carbonyl group, Tyr194 alcohol and Glu53 carboxylate. The His121 lateral chain and a conserved water molecule inside the cavity are located close to the alcohol and therefore might also interact with the glycerol function and participate to the MAGL selectivity for monoacylglycerols.

To further illustrate the contribution provided by this alcohol-binding pocket to the substrate specificity, MAGL and the aryl esterase from *Pseudomonas fluorescens* were compared.[29] In the latter, in which substrates are esters with a small acyl group and an aryl-alcohol moiety, the small pocket corresponding to this area is much more hydrophobic and is bordered by aromatic or aliphatic residues. Therefore, this allows interaction with the aryl group of the substrate.

MAGL was reported to hydrolyse 1-OG and 2-OG at similar rates,[37] and docking of 2-AG allows to understand this lack of selectivity. In cases in which the fatty acyl chain is bound in the 2 position, the glycerol moiety does not entirely fill up the hydrophilic cavity, which extends somewhat deeper in the active site (Figure 4). Therefore, the glycerol group of 1-OG can freely be accommodated in the same pocket without encountering a steric hindrance, and stretches to the bottom of the cavity (Figure S4).

Another interesting feature consists of a small opening of about 5 Å diameter connecting the active site to the outside of the protein (Figures 1 and 4). The aperture forms thanks to the original architecture of the MAGL cap domain, more precisely the loops connecting α4 to α5 and α5 to α6 helices, and the last portion of the α5 helix. This small channel, coated by Pro178 to Ser181, Leu184, Tyr194, Asn195, Arg202 and Ala203, and perpendicular to the trajectory leading from the hydrophilic pocket to the membrane binding site, could constitute an optimal exit door for the glycerol moiety, released after 2-AG hydrolysis.

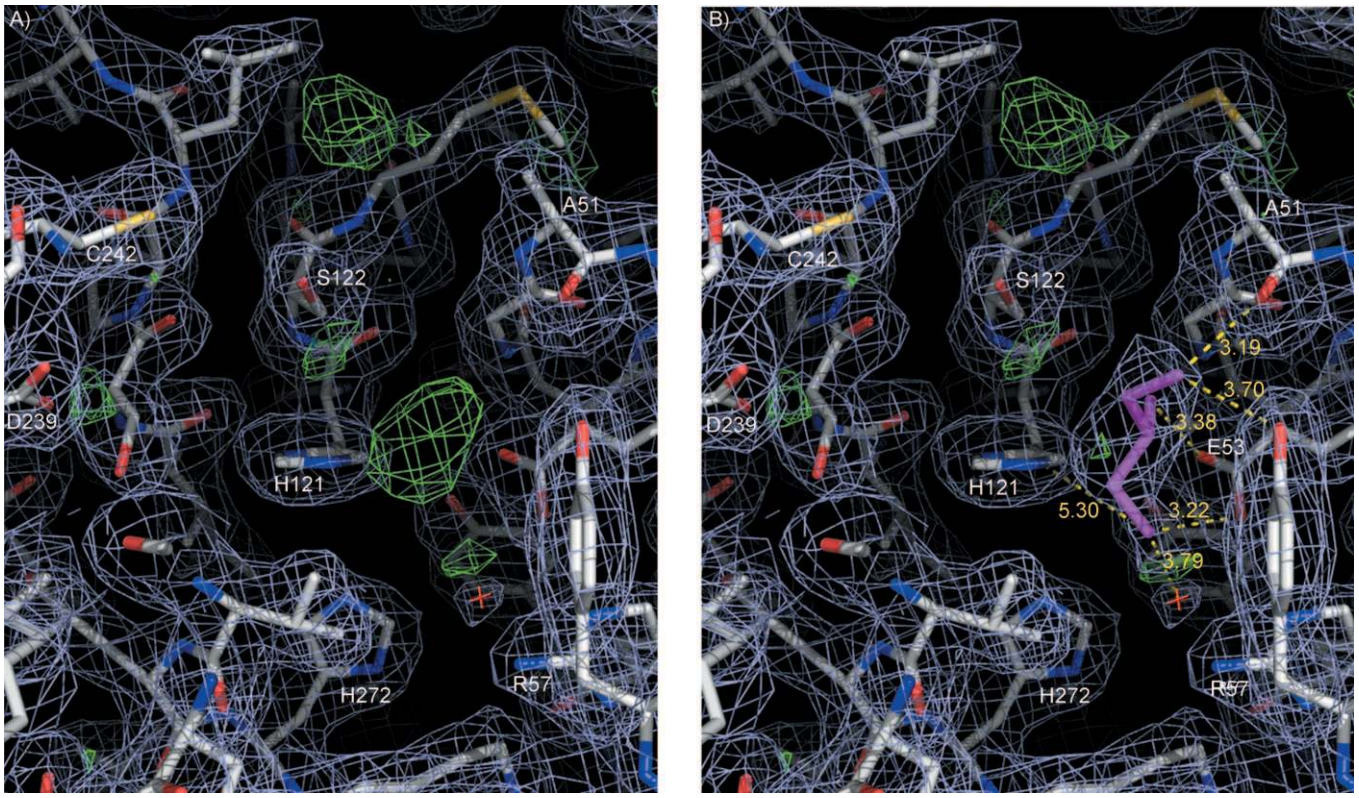

Figure 5. Electron density in MAGL active site. A glycerol molecule is bound in the alcohol-binding pocket. A) Electron density map ($2F_o-F_c$, blue mesh, contoured at 1σ; F_o-F_c, green mesh, contoured at 3σ) showing a residual electron density in the alcohol-binding pocket. This residual density in the experimental map is most probably due to a glycerol molecule, used as a cryoprotectant. B) This residual electron density disappears when a glycerol molecule is included in the model. Distances between glycerol oxygen atoms and the amino acids properly placed to establish hydrogen bonds with are indicated in angstroms. A water molecule is represented by a red cross.

Towards the rational design of MAGL inhibitors

The most potent MAGL inhibitors reported to date are JZL184 and the 2,5-regioisomer of the Eli-Lilly compound LY2183240 (compound **1**). JZL184 is more potent than compound **1**, with

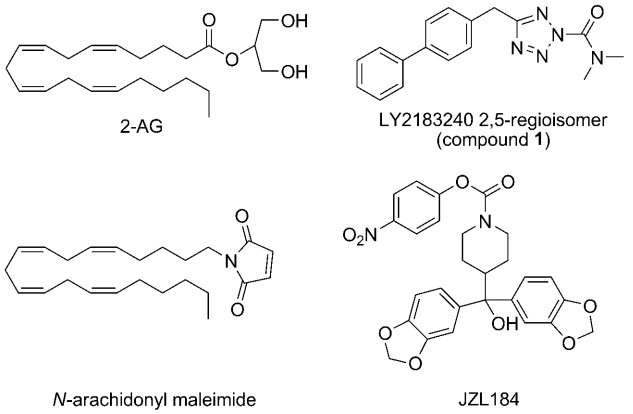

IC_{50} values of 8 nM and 20 nM, respectively.[13,38] Unlike compound **1**, JZL184 also offers the advantage of an improved selectivity for MAGL versus FAAH. We docked these two compounds in the MAGL cavity, both in the tetrahedral intermediate state (Figure 6). The small AM6701 dimethylamino group fails to properly fill the hydrophilic cleft, and it is likely that increasing the size and hydrophilicity of this moiety could help increase inhibitory potency. On the contrary, the *p*-nitrophenyl group of JZL184 fits better in this cavity than the corresponding substituent of compound **1**. This could reflect the improved inhibitory potency reported for JZL184 compared to compound **1**. Alternative conformations of the JZL184 bis(methylene-3,4-dioxyphenyl) group were found to coexist. This permissiveness is allowed by the width of the active site entrance, which also provides a rational explanation for the reported JZL184 selectivity. Indeed, while its wide active site access allows MAGL to accommodate the bulky bis(methylene-3,4-dioxyphenyl) group, FAAH displays much narrower cavities into which JZL184 can hardly slip.

***N*-arachidonylmaleimide binding**

Four cysteines are present in human MAGL, three of which are located in the vicinity of the catalytic site (Cys201, Cys208, Cys242). Since the first purification of monoacylglycerol lipase, it is known that sulfhydryl-reacting compounds inactivate MAGL.[37] Saario and colleagues then reported the use of a series of maleimide-based compounds as inhibitors, with *N*-arachidonylmaleimide (NAM) as the most potent representative. Based on a homology model, they proposed an inhibition mechanism involving a Michael addition of the maleimide moiety on either the Cys208 or Cys242 residue.[27] By mutating rat MAGL residues corresponding to Cys208 and 242, a subsequent study pointed to Cys242 as the crucial residue responsible for this inactivation.[39] However, the relief of inhibition generated by the C242A mutation remained modest (pIC_{50} on WT rat MAGL = 5.55 vs. 5.19 for the mutated enzyme). The present crystal structure reveals that Cys201 is located near the catalytic site, in a loop connecting α5 to α6 helices. Accessible from the inside of the catalytic site, Cys201 therefore constitutes a good candidate for the regulation of MAGL activity. On the contrary, Cys208, residing in the α6 helix, points towards the outside of the protein, and hence seems incorrectly placed to react with NAM. To clarify this, we decided to mutate these three cysteines, and to measure the inhibitory potential of NAM (Figure 7).

As a result, we reproduced here the very slight decrease in NAM sensitivity previously observed by Zvonok in the C242A mutant. We also noticed an increase in the inhibiting power in the C208A and C208A/C242A mutants (pIC_{50} for WT = 6.27 ± 0.03; C242A = 6.11 ± 0.04; C208A = 6.64 ± 0.04; C208A/C242A = 6.48 ± 0.03). This leads to several conclusions. First, when Cys208 is absent, NAM is more available to inhibit MAGL through one or several other cysteine(s). Second, the decrease in NAM inhibitory potency in the C242A mutant reflects the binding of NAM to Cys242, but the weakness of this effect suggests that this event is not a determining factor and only leads to a modest inhibition of activity. Last, the overall increase in pIC_{50} in the C208A/C242A double mutant is a definite evidence that another cysteine is more crucial than Cys208 or Cys242 for MAGL inhibition by NAM.

Indeed, C201A simple mutant showed a substantial decrease in the inhibitory potential (pIC_{50} for C201A = 5.38 ± 0.14). Moreover, NAM was unable to completely inhibit the activity of this mutant enzyme, as about 35% activity remained at 10^{-4} M. C201A/C208A/C242A triple mutant did not display significant inhibition by NAM; this reflects the fact that the residual inhibition observed in the C201A mutant involves the Cys242 residue, located only 4 Å away from the nucleophilic serine.

Interestingly, during the writing of this paper, King and colleagues reported a similar decrease in NAM sensitivity in a rat MAGL C201A simple mutant.[40] Therefore, taken together, these results are definitely more in accordance with an inhibition mainly involving Cys201, although an alternative, albeit much less decisive, mechanism might be possible, involving a binding to Cys242.

Conclusions

Recent data suggest a tissue-specific function for MAGL. Beside its crucial role in the termination of 2-AG synaptic signaling in the brain, it is assumed to be responsible for an alternative function in the metabolism of triglycerides. In the adipose tissue, it is thought to follow the action of adipose triglyceride lipase (ATGL) and hormone sensitive lipase (HSL) to complete the total hydrolysis of triglycerides to fatty acids and glycerol.[41] In the liver, MAGL could be involved in the mobilization of triglycerides for secretion.[42]

The crystal structure described herein reveals how MAGL has evolved to distinguish itself from the huge number of proteins that belong to the α/β hydrolase fold superfamily. These adaptations mainly arise from remodeling of the architecture and

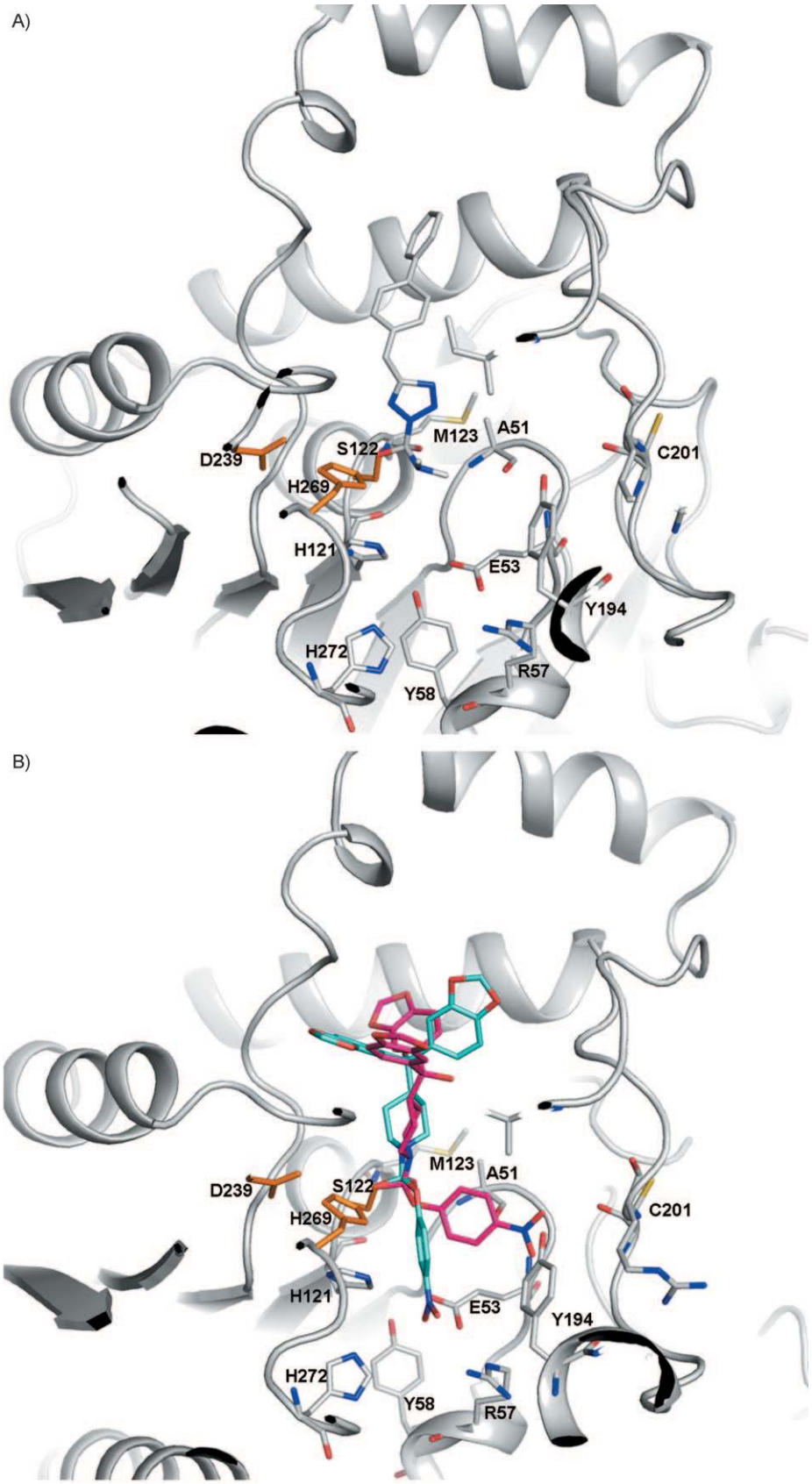

Figure 6. Docking of the A) 2,5-isomer of LY2183240 (compound **1**) and B) JZL184 in the active site of MAGL. Both compounds are bound in the tetrahedral intermediate state to Ser122. Two main conformations were found for the latter.

properties of the cap domain; this allows interaction with membranes and the creation of a mix hydrophobic/hydrophilic environment optimal for the accommodation of monoacylglycerols in the catalytic site. Inside the catalytic site, targeting Cys201 and Cys242 provides the means to regulate MAGL activity.

As mentioned above, MAGL is a hot therapeutic target, because the design of selective and potent inhibitors could provide unique tools to interfere with 2-AG degradation and to finely modulate the endocannabinoid signal. Considering the very hydrophobic nature of the acyl-binding pocket and the need to design drug-like inhibitors of MAGL, exploiting the small polar alcohol-binding pocket revealed by our work constitutes a promising approach to overcome the problems associated with the use of lipophilic compounds like *N*-arachidonylmaleimide.[27]

Thus, besides contributing to an in depth knowledge of the routes that govern lipid metabolism and regulate endocannabinoid levels, the tridimensional structure of human monoacylglycerol lipase paves the way for future medicinal chemistry endeavours aimed at the design of new and valuable drugs exploiting 2-AG transmission.

Experimental Section

MAGL cloning and expression: Human MAGL was produced in the *E. coli* Rosetta strain, as previously described by our group, with only minor modifications.[43] Purification was performed by a combination of streptactin and ion metal affinity chromatography. However, after the second purification step, MAGL sample was loaded once again onto streptactin column, washed with buffer A (15 mM Hepes, 1 mM dithiothreitol, pH 8.2), and eluted with the

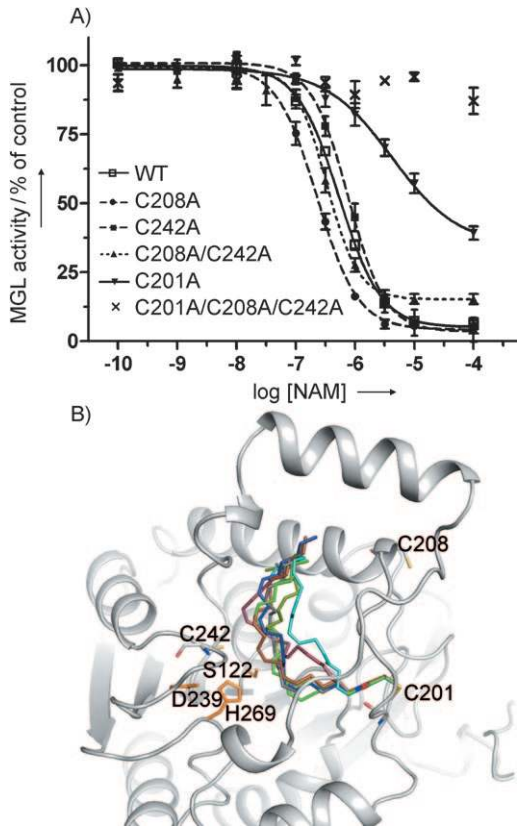

Figure 7. NAM inhibits human MAGL by targeting Cys201. A) Dose-dependent inhibition of wild-type and mutant MAGL by NAM. Values are expressed as percent of control and represent mean ±SEM of at least four experiments done in duplicate. B) Docking of NAM in the active site of MAGL, bound to Cys201. The main conformations found by using Gold software are represented with different colours. Catalytic triad is coloured in orange, and Cys201, Cys208 and Cys242 are represented.

same buffer supplemented with desthiobiotin (2.5 mM). Glycerol (10%, *m/v*) was then added, and protein was concentrated to ~15 mg mL^{-1}.

For selenomethionyl MAGL production, cultures were grown in minimal media. At an O.D. of 0.6, a mixture of amino acids was added (L-threonine 100 mg L^{-1}, L-lysine 100 mg L^{-1}, L-phenylalanine 100 mg L^{-1}, L-leucine 50 mg L^{-1}, L-isoleucine 50 mg L^{-1} and L-valine 50 mg L^{-1}) and the culture was incubated for 1 h at 37 °C. Following this, protein production and purification were performed as for the native MAGL. It is noteworthy to mention that lower yields were obtained for selenomethionyl compared to native MAGL production (typically 1 mg and 5 mg per liter of culture medium, respectively).

Crystallization: crystals were grown by the hanging drop and under oil crystallization methods. For native MAGL, best crystals were obtained by mixing concentrated MAGL (1 μL) with crystallization mixture (1 μL, 70 mM sodium cacodylate, 45% 2-methyl-2,4-pentanediol, pH 4.5) in the presence of hexaethyleneglycol monodecylether (0.1 mM). Crystals grew from a precipitate, and typically reached their maximum size after incubation at room temperature during one to two weeks. For the heavy metal soaking experiment, crystals, obtained by mixing protein solution (1 μL) with of crystallization mixture (1 μL, 70 mM sodium cacodylate, 40% 2-methyl-2,4-pentanediol, pH 3.0) were soaked for 45 min in mother liquor supplemented with PEG 8k (5%) and $KAu(CN)_2$ (10 mM). Crystallization of the selenomethionyl derivative was achieved by mixing protein solution (1 μL) with of crystallization mixture (1 μL, 70 mM sodium cacodylate, 35% 2-methyl-2,4-pentanediol, pH 5.0) in the presence of lauryl dimethylamine *N*-oxide (LDAO, 1–3 mM). It has to be noted that the presence of detergent was absolutely required for the crystallization of this MAGL derivative, as no nucleation occurred when LDAO was omitted.

Data collection and model building: Diffraction data were collected at the European Synchrotron Radiation Facility (ESRF; BM30A and ID29) at 100 K. The data were processed by using the XDS program.[44] First crystals diffracted to 3 Å. After several unsuccessful attempts to solve the structure by molecular replacement, the structure was solved using a combination of SIRAS (single isomorphous replacement with anomalous signal) and SAD (single wavelength anomalous diffraction) by using SHARP/Autosharp software.[45,46] Following manual building of the human MAGL model in the experimental electron density map (Figure S1), crystals with improved resolution were grown, and the coordinates of the final human MAGL model at 2.2 Å have been deposited in the protein data bank (PDB ID: 3HJU). Further details are available in the Supporting Information.

Mutants construction: MAGL mutants genes were obtained by following standard molecular biology protocols and were entirely sequenced to confirm the absence of unwanted mutations. Production was carried out as described for the wild-type enzyme. However, after expression of the proteins, *E. coli* pellet was harvested, resuspended in a Tris buffer (50 mM Tris, 200 mM NaCl, 0.1% LDAO, pH 9.5) and submitted to sonication to disrupt the cells. The lysate was then centrifuged at 10 000 *g* for 35 min and the supernatant containing WT or mutant MAGL was frozen at −80 °C until use. A control culture not bearing MAGL encoding plasmid confirmed the absence of endogenous *E. coli* 2-oleoylglycerol hydrolase activity.

MAGL esterase activity assay: MAGL activity was measured by following 2-oleoyl glycerol (2-OG) hydrolysis, as previously described.[21] Briefly, 2-OG (10 μM; [^{3}H]-2-OG 50 000 dpm, American Radiolabeled Chemicals, St. Louis, MO, USA) was incubated at 37 °C for 10 min in the presence of soluble fraction of *E. coli* lysate (50 mM Tris buffer, pH 8.0; 200 μL of total volume assay) and the inhibitor (10 μL, dissolved in DMSO). The reaction was stopped by adding methanol/chloroform (1:1; 400 μL), and the radioactivity was measured in the upper aqueous phase by liquid scintillation counting. *N*-Arachidonylmaleimide (NAM) was purchased from Cayman Chemical (Ann Arbor, MI, USA). The results are expressed as percent of control activity for the inhibitor evaluation experiments. GraphPad prism was used to treat the data and to analyse the dose-response curves. Inhibitor potency is expressed as pIC_{50} values ±standard error of the mean (sem).

For additional materials and methods see the Supporting Information.

Acknowledgements

The authors would like to greatly thank Dr. Giulio G. Muccioli for helpful discussions regarding all aspects of this work, as well as Dany Van Elder for technical assistance during data collection at the ESRF. This work was supported by a FRFC (FNRS) no. 2.4654.06 grant. Use of the FIP/BM30a beamline of ESRF for the MAGL structure project was supported by the Fonds de la Recherche Scientifique under Contract IISN 4.4505.00.

Keywords: crystal structures · enzymes · inhibitors · monoacylglycerol lipase · monoglyceride lipase · *N*-arachidoyl maleimide

[1] L. A. Matsuda, S. J. Lolait, M. J. Brownstein, A. C. Young, T. I. Bonner, *Nature* **1990**, *346*, 561 – 564.
[2] S. Munro, K. L. Thomas, M. Abu-Shaar, *Nature* **1993**, *365*, 61 – 65.
[3] W. A. Devane, L. Hanus, A. Breuer, R. G. Pertwee, L. A. Stevenson, G. Griffin, D. Gibson, A. Mandelbaum, A. Etinger, R. Mechoulam, *Science* **1992**, *258*, 1946 – 1949.
[4] R. Mechoulam, S. Ben Shabat, L. Hanus, M. Ligumsky, N. E. Kaminski, A. R. Schatz, A. Gopher, S. Almog, B. R. Martin, D. R. Compton, *Biochem. Pharmacol.* **1995**, *50*, 83 – 90.
[5] T. Sugiura, S. Kondo, A. Sukagawa, S. Nakane, A. Shinoda, K. Itoh, A. Yamashita, K. Waku, *Biochem. Biophys. Res. Commun.* **1995**, *215*, 89 – 97.
[6] R. I. Wilson, R. A. Nicoll, *Nature* **2001**, *410*, 588 – 592.
[7] V. Di Marzo, *Nat. Rev. Drug Discovery* **2008**, *7*, 438 – 455.
[8] S. Pillarisetti, C. W. Alexander, I. Khanna, *Drug Discovery Today* **2009**, *14*, 1098 – 1111.
[9] S. M. Saario, J. T. Laitinen, *Basic Clin. Pharmacol. Toxicol.* **2007**, *101*, 287 – 293.
[10] B. Szabo, M. J. Urbanski, T. Bisogno, V. Di Marzo, A. Mendiguren, W. U. Baer, I. Freiman, *J. Physiol.* **2006**, *577*, 263 – 280.
[11] N. Stella, P. Schweitzer, D. Piomelli, *Nature* **1997**, *388*, 773 – 778.
[12] G. Hohmann, R. L. Suplita, N. M. Bolton, M. H. Neely, D. Fegley, R. Mangieri, J. F. Krey, J. M. Walker, P. V. Holmes, J. D. Crystal, A. Duranti, A. Tontini, M. Mor, G. Tarzia, D. Piomelli, *Nature* **2005**, *435*, 1108 – 1112.
[13] J. Z. Long, W. Li, L. Booker, J. J. Burston, S. G. Kinsey, J. E. Schlosburg, F. J. Pavón, A. M. Serrano, D. E. Selley, L. H. Parsons, A. H. Lichtman, B. F. Cravatt, *Nat. Chem. Biol.* **2009**, *5*, 37 – 44.
[14] M. Gokoh, S. Kishimoto, S. Oka, M. Mori, K. Waku, Y. Ishima, T. Sugiura, *Biochem. J.* **2005**, *386*, 583 – 589.
[15] S. Oka, S. Ikeda, S. Kishimoto, M. Gokoh, S. Yanagimoto, K. Waku, T. Sugiura, *J. Leukocyte Biol.* **2004**, *76*, 1002 – 1009.
[16] M. Melis, G. Pillolla, T. Bisogno, A. Minassi, S. Petrosino, S. Perra, A. L. Muntoni, B. Lutz, G. L. Gessa, G. Marsicano, V. Di Marzo, M. Pistis, *Neurobiol. Dis.* **2006**, *24*, 15 – 27.
[17] C. J. Hillard, *J. Pharmacol. Exp. Ther.* **2000**, *294*, 27 – 32.
[18] K. Nithipatikom, M. P. Endsley, M. A. Isbell, C. E. Wheelock, B. D. Hammock, W. B. Campbell, *Biochem. Biophys. Res. Commun.* **2005**, *332*, 1028 – 1033.
[19] D. Melck, L. De Petrocellis, P. Orlando, T. Bisogno, C. Laezza, M. Bifulco, V. Di Marzo, *Endocrinology* **2000**, *141*, 118 – 126.
[20] M. Karlsson, J. A. Contreras, U. Hellman, H. Tornqvist, C. Holm, *J. Biol. Chem.* **1997**, *272*, 27218 – 27223.
[21] T. P. Dinh, D. Carpenter, F. M. Leslie, T. F. Freund, I. Katona, S. L. Sensi, S. Kathuria, D. Piomelli, *Proc. Natl. Acad. Sci. USA* **2002**, *99*, 10819 – 10824.
[22] J. L. Blankman, G. M. Simon, B. F. Cravatt, *Chem. Biol.* **2007**, *14*, 1347 – 1356.
[23] T. Bisogno, G. Ortar, S. Petrosino, E. Morera, E. Palazzo, M. Nalli, S. Maione, V. Di Marzo, *Biochim. Biophys. Acta Mol. Cell Biol. Lipids* **2009**, *1791*, 53 – 60.
[24] T. P. Dinh, S. Kathuria, D. Piomelli, *Mol. Pharmacol.* **2004**, *66*, 1260 – 1264.
[25] M. H. Bracey, M. A. Hanson, K. R. Masuda, R. C. Stevens, B. F. Cravatt, *Science* **2002**, *298*, 1793 – 1796.
[26] B. Hofmann, S. Tolzer, I. Pelletier, J. Altenbuchner, K. H. van Pee, H. J. Hecht, *J. Mol. Biol.* **1998**, *279*, 889 – 900.
[27] S. M. Saario, O. M. Salo, T. Nevalainen, A. Poso, J. T. Laitinen, T. Järvinen, R. Niemi, *Chem. Biol.* **2005**, *12*, 649 – 656.
[28] S. M. Saario, A. Poso, R. O. Juvonen, T. Järvinen, O. M. Salo-Ahen, *J. Med. Chem.* **2006**, *49*, 4650 – 4656.
[29] J. D. Cheeseman, A. Tocilj, S. Park, J. D. Schrag, R. J. Kazlauskas, *Acta Crystallogr. Sect. D Biol. Crystallogr.* **2004**, *60*, 1237 – 1243.
[30] F. Elmi, H. T. Lee, J. Y. Huang, Y. C. Hsieh, Y. L. Wang, Y. J. Chen, S. Y. Shaw, C. J. Chen, *J. Bacteriol.* **2005**, *187*, 8470 – 8476.
[31] A. Roussel, N. Miled, L. Berti-Dupuis, M. Riviere, S. Spinelli, P. Berna, V. Gruber, R. Verger, C. Cambillau, *J. Biol. Chem.* **2002**, *277*, 2266 – 2274.
[32] M. Karlsson, K. Reue, Y. R. Xia, A. J. Lusis, D. Langin, H. Tornqvist, C. Holm, *Gene* **2001**, *272*, 11 – 18.
[33] M. Brzozowski, U. Derewenda, Z. S. Derewenda, G. G. Dodson, D. M. Lawson, J. P. Turkenburg, F. Bjorkling, B. Huge-Jensen, S. A. Patkar, L. Thim, *Nature* **1991**, *351*, 491 – 494.
[34] M. P. Egloff, F. Marguet, G. Buono, R. Verger, C. Cambillau, H. van Tilbeurgh, *Biochemistry* **1995**, *34*, 2751 – 2762.
[35] H. van Tilbeurgh, Y. Gargouri, C. Dezan, M. P. Egloff, M. P. Nésa, N. Ruganie, L. Sarda, R. Verger, C. Cambillau, *J. Mol. Biol.* **1993**, *229*, 552 – 554.
[36] C. Eydoux, S. Spinelli, T. L. Davis, J. R. Walker, A. Seitova, S. Dhe-Paganon, A. De Caro, C. Cambillau, F. Carrière, *Biochemistry* **2008**, *47*, 9553 – 9564.
[37] H. Tornqvist, P. Belfrage, *J. Biol. Chem.* **1976**, *251*, 813 – 819.
[38] G. Ortar, M. G. Cascio, A. S. Moriello, M. Camalli, E. Morera, M. Nalli, V. Di Marzo, *Eur. J. Med. Chem.* **2008**, *43*, 62 – 72.
[39] N. Zvonok, L. Pandarinathan, J. Williams, M. Johnston, I. Karageorgos, D. R. Janero, S. C. Krishnan, A. Makriyannis, *Chem. Biol.* **2008**, *15*, 854 – 862.
[40] A. R. King, A. Lodola, C. Carmi, J. Fu, M. Mor, D. Piomelli, *Br. J. Pharmacol.* **2009**, *157*, 974 – 983.
[41] R. Zechner, P. C. Kienesberger, G. Haemmerle, R. Zimmermann, A. Lass, *J. Lipid Res.* **2009**, *50*, 3 – 21.
[42] S. H. Chon, Y. X. Zhou, J. L. Dixon, J. Storch, *J. Biol. Chem.* **2007**, *282*, 33346 – 33357.
[43] G. Labar, C. Bauvois, G. G. Muccioli, J. Wouters, D. M. Lambert, *ChemBioChem* **2007**, *8*, 1293 – 1297.
[44] W. Kabsch, *J. Appl. Crystallogr.* **1993**, *26*, 795 – 800.
[45] G. de La Fortelle, G. Bricogne, *Methods Enzymol.* **1997**, *276*, 472 – 494.
[46] C. Vonrhein, E. Blanc, P. Roversi, G. Bricogne, *Methods Mol. Biol.* **2007**, *364*, 215 – 230.
[47] D. P. Tieleman, H. J. C. Berendsen, *Biophys. J.* **1998**, *74*, 2786 – 2801. http://moose.bio.ucalgary.ca/

Received: October 9, 2009
Published online on December 2, 2009

